Research Square

Preprints are preliminary reports that have not undergone peer review.
They should not be considered conclusive, used to inform clinical practice,
or referenced by the media as validated information.

Longitudinal variation in log properties of Pinus radiata in northern Tasmania: predicting log stiffness using resistance drilling

Geoffrey M. Downes
geoff.downes@forestquality.com

Forest Quality Pty. Ltd
Robert Musk
Timberlands Pacific
Kaine Arkley
Timberlands Pacific
Vilius Gendvilas
University of the Sunshine Coast
David Lee
University of the Sunshine Coast

Research Article

Keywords: log stiffness, radiata pine, resistance drilling, wood variability, wood quality

Posted Date: May 25th, 2026

DOI: https://doi.org/10.21203/rs.3.rs-9775173/v1

License: This work is licensed under a Creative Commons Attribution 4.0 International License. Read Full License

Additional Declarations: No competing interests reported.

Version of Record: A version of this preprint was published at European Journal of Wood and Wood Products on October 10th, 2026. See the published version at https://doi.org/10.1007/s00107-026-02487-1.

Abstract

• Within-stem and between stem variation in log stiffness in 591 logs of 2.5 meters in length were assessed from 65 *Pinus radiata* D.Don trees, sampled across 13 plots of 5 individual trees, representing 7 forests in northern Tasmania, Australia.

• Average log stiffness was significantly affected by stand age, stocking and basal area.

• Within stems, a consistent pattern of increasing then decreasing modulus of elasticity and acoustic resonance was observed with highest stiffness values between 5 and 15 metres above ground. The general pattern was consistent among sites with between site variance predominantly in the y-intercept value.

• Resi-predicted basic density was significantly correlated with log modulus of elasticity (MOE), with the strength of the relationship varying markedly among sampling points based on position within the stem.

• Multiple regression and random forest models, based on traits extracted from the Resi trace, were found to better account for variance in log MOE, compared to Resi-predicted basic density alone. Random forest models were able to explain 56% of the variation at the individual tree level; this improved to 88% at the site level.

Introduction

Timber production via plantation forestry is a relatively slow process that transcends shifts in government policy that affect its efficiency, focus and profitability. Over recent decades general economic policy paradigms have favoured the dis-aggregation of the forest supply chain into, broadly speaking, growers, processors and manufacturers. A consequence of this has been the financial incentive for growers to shorten rotation lengths, enhancing the return on investment via a primary focus on improved stem diameter and volume growth rates.

The variation in plantation softwood wood properties within the stem has been a major focus of research (Lachenbruch et al. 2011; Gil-Moreno et al. 2023; Evans 1994) over decades with a well established pattern of increasing basic density from pith to bark, together with the associated decrease in microfibril angle (Moore et al. 2014; Pot et al. 2025a), resulting in a pattern of radial improvement in structural wood quality. In general terms this is understood in terms of juvenile (low quality) wood near the pith and mature (better quality) wood towards the bark. Consequently a reduction in rotation length, as optimal log diameters are achieved at earlier ages, results in an increase in the proportion of lower quality juvenile wood in logs (Kennedy 1995; Pot et al. 2025b). Longitudinal variation in log properties, which is markedly affected by the radial variation patterns, has also been studied extensively (Donaldson et al. 2004; Xu et al. 2004; Watt et al. 2011; Waghorn et al. 2007; Beets et al. 2018), having the advantage that variation can more easily be partitioned into logs of varying quality according to their within-stem position. Understanding and quantifying the effects of site, rotation length and management on these longitudinal patterns of wood property change can assist the valuation of stands by basing value on additional stem features as well as volume and form.

Globally, resistance drilling (DR) using Resi/Resistograph-type instruments is increasingly applied for rapid standing-tree wood property assessment, predominantly wood density, supporting applications in breeding, inventory, and forest resource characterisation across North America, Europe, South America, and Asia (Fundova et al. 2018, 2019; Vlad et al. 2022; Šilinskas et al. 2026; Icel 2025; Singh et al. 2023; Todoroki et al. 2021; Yao et al. 2024; Barría et al. 2017; Bouffier et al. 2008; Pádua et al. 2019; Gwaze and Stevenson 2008; Isik and Li 2003; Eckard et al. 2010). Related studies have also explored the use of drilling resistance for stiffness/MOE assessment, either directly or in combination with acoustic methods (Eckard et al. 2010; Fundova et al. 2019; Sharapov et al. 2019).

In Australia DR is now commonly used in forestry operations for standing-tree wood quality assessment and pre-harvest resource characterisation (Bailleres et al. 2019; Downes and Lausberg 2016; Downes et al. 2020; Kumar et al. 2021; Downes et al. 2022; Gendvilas, Lee, et al. 2024). Growers seek to understand the variability in value across their estates and gain commercial advantage from supplying logs of known properties to their customers. Previously basic density assessments via pilodyn (Watt et al. 1996) or outerwood increment coring has been the common assessment approach (Cown and Hutchison 1983). However, this has been too expensive for wide spread commercial use in pre-harvest assessments. Resistance drilling, combined with web-based processing of traces, offers a demonstrably low-cost option that is sufficiently precise and accurate for the various metrics produced (under and over-bark diameter, basic density) (Downes and Lee 2024; Downes et al. 2018; Gendvilas, Lee, et al. 2024). A major development goal has been to estimate or predict log stiffness (modulus of elasticity - MOE) from DR data, typically using basic density as a surrogate, but increasingly utilising regression models that include additional metrics extracted from the Resi trace related to acoustic wave velocity (AWV) variance (Downes and Lausberg 2016) as assessed using the FibreGen HM200 instrument (FibreGen, Christchurch, New Zealand).

To better utilise the efficiency of DR in the collection of wood property data, the longitudinal variation in actual log stiffness was assessed in 65 trees representing 13 plots from 7 different forests. The longitudinal patterns in stiffness with stems and between forests was examined, and how this related to the pattern in Resi-determined basic density and stiffness. Two objectives were pursued:

- To compare variation among mature stands in actual log MOE and how longitudinal variation in log stiffness compared between stands
- To develop models that could predict log MoE based on metrics that could be extracted from individual Resi traces, where these metrics required little or no human intervention to extract.

Methods

As part of a larger project exploring the application of resistance drilling to mid-rotation wood property assessment (Lee et al. 2024), Timberlands Pacific (TPPL) felled trees across a range of plots to define in-house taper equations and collect basic density and modulus of elasticity (MOE) data to model within-tree variation from breast height measurements. The field work objectives were:

- Collect along the stems, over and under-bark diameter observations to support the updating of taper models deployed in yield tables.
- Collect wood property observations at 2.5 metre intervals along the stem (Resi, HM200, green density) to develop models of within-tree wood property variation.

Tree selection

From the current planned thinning and clearfall operations, seven sites across northern Tasmania were selected for sampling. These represented a range of age, altitude, longitude, stocking, and site index (Table 1) metrics. The stands represented a range of productivity with respect to annual average volume production. Stocking within the clearfall stands ranged from 450 to 1200 sph.

Table 1
Forest descriptive metrics.

Site	Plot	Age	BasalArea	TopHeight	Stocking	Elevation
806	1	27.2	67.4	38.8	450	350
806	2	27.2	76.7	39.8	475	355
807	1	25.3	64.4	34.4	625	484
807	2	25.3	63.8	34.4	525	470
810	2	25.2	101.	38.2	920	260
821	1	12.7	41.1	21.5	1350	104
821	2	13.7	47.5	22.1	900	100
828	1	26.9	72.5	36.0	628	180
828	2	26.9	66.9	36.2	485	187
830	1	15.9	63.7	23.9	1350	590
830	2	15.9	50.5	25.7	1100	590
833	1	13.6	62.7	21.3	1600	464
833	2	13.7	37.4	21.5	900	450
(Note: no log data available from Plot 1 of site 810)						

Data collection

In total, 65 trees were felled over a 12-month period from 13 plots covering the seven selected stands. Figure 1 illustrates the sampling scheme adopted. Two circular plots, targeting 20 trees were sampled within each stand, with each plot at least 10 m from the stand edge. Plot area was approximately 0.4 ha. The diameter over bark at breast height (DBHOB) at 1.3m above ground from each tree was recorded using a diameter tape. Each tree was sampled using an IML Resi PD-400 (IML System GmbH, Wiesloch, Germany) instrument (Gendvilas, Lee, et al. 2024) to collect two orthogonal bark-to-bark traces using the sampling conditions of 3500 rpm and 200 $cm.min^{-1}$ feed speed.

Five trees, each from a separate quintile of the diameter distribution, from each plot were selected for felling and wood property and taper assessment. Selections were made to avoid trees that exhibited forking or ramicorns, lean greater than 10^{o}, scarring, broken tops, very suppressed or abnormal taper. Prior to felling the stem was marked at 0.2, 0.7 and 1.3m above ground. Trees were felled away from the plot centre to avoid stems crossing and facilitate further assessment. Stems were delimbed and stump height recorded.

Each stem was marked at 2.5 m from the base to merchantable height. If a band was located on a whorl (stem swelling) the position was adjusted to clear stem without affecting the location of the next band. Two orthogonal Resi traces (horizontal and vertical) were collected at each band Fig. 2 to assess variation in basic density as per (Gendvilas, Lee, et al. 2024).

Each stem was cut at the marked locations to yield individual logs and the acoustic wave velocity (AWV) of the log recorded using the Director HM200™ instrument (FibreGen, Christchurch, New Zealand). A five centimetre thick cross section was removed from each band, and at the 0.2, 0.7 and 1.3m points, bark removed and underbark diameter estimated from the geometric mean of two orthogonal ruler measurements from the approximate minor and major axes of the discs. All discs were processed for assessment of green weight and volume for the calculation of green density.

As AWV values vary with moisture content, the inclusion of green density enables the calculation of log MoE allowing for this source of variance. Overall 591 logs of 2.5m length were generated for this study, and average of 9 logs per tree.

Data analyses

Resi traces were read into the web portal (https://forestquality.shinyapps.io/FWPA-5/ accessed 11 Feb 2025) and processed to generate Resi project files ("*.Resi" in rds format), containing individual trace data and the summary information generated for each trace. Resi traces were baseline corrected and checked for correct type allocation pith-to-bark (P-B) or bark-to-bark (B-B) as per Downes (2023) and cambial and pith positions were suitably located. Disc basic density was estimated from each height position using mean area-weighted values of each of the 4 radial under-bark portions from the two Resi traces. Trace processing generated a range of variables derived from the Resi trace to explore their potential to develop an improved prediction model for acoustic wave velocity (AWV) and log stiffness (log MoE). Log stiffness was calculated using the following equation, where green density was determined from the cross-section discs sampled from either end of the log.

$$LogMOE = AWV^2 * GreenDensity$$

Variation in whole tree MoE was assessed at the plot mean level, using linear regression and linear mixed effects modelling via the "lmer" function in the lme4 package (Bates et al. 2015), where tree MOE was calculated as a volume weighted mean of all logs within a given stem.

Model development for prediction of log MOE from Resi data

To explore the potential of predicting log MOE from a Resi trace more precisely than allowed by the relationship with basic density alone, a range of variables were extracted from the Resi data that were considered to offer some potential to describe the variance that might be partly related to microfibril angle variation independent of its empirical relationship with basic density. Following Dahlen et al. (2023) a four parameter logistic function defined by Ratkowsky (1990) was used to capture the general pattern of radial variation. The form of the equation is below.

$$WoodProperty\,(x) = B + \frac{A - B}{1 + exp\left(\frac{C - x}{D}\right)}$$

Curves were fitted to 1715 Resi traces obtained in this study using the nlsLM function from the "minpack.lm" R package (Elzhov et al. 2023) and values for each of the four parameters (A,B,C & D) defined.

From a biological perspective these parameters are indicative of the following:

- A: mature wood plateau close to the bark
- B: low density value close to the pith
- C: radial position of the point where the density exceeds the mean of A and B
- D: rate of change in the radial trajectory of density at C

Table 2 lists and briefly describes 29 variables extracted from each Resi trace. All traces were processed as individual pith-to-bark radii where radial position was expressed as a percentage. At this stage of evaluation, where the Resi trace was a complete diameter (bark-to-bark) consisting of opposing diameters (entry and exit), an average radius was constructed by first converting each radius (entry and exit) to percentage radial intervals add averaging them. The variables were defined to describe aspects of some extent of the radial variation.

Table 2
Resi-derived variables for use in regression model development

Variable Name	Description	Transformation
DOB	Over-bark diameter	none
UBDIA	Under-bark diameter	none
CoreDensity	pith-to-bark basic density	none
DiscDensity	Area-weighted basic density	none
A	Upper asymptote of sigmoid curve	none
B	Lower asymptote of sigmoid curve	none
C	Position of midpoint between A and B	sqrt
D	Rate of change of slope at C	ln
RPD	Ratio of performance to deviation of the fitted curve (RPD = sd/SEP)	none
Range	Difference between A and B	none
pResidualMean	Mean of the residuals of the fitted curve	none
pResidualSD	Standard deviation of the residuals of the fitted curve	none
pDensitySD	Standard deviation in the density values across the radius	none
pDensity.1DerMean	Mean of the first derivative of the Resi trace	none
pDensity.1DerSD	Standard deviation of the first derivative of the Resi trace	none
pCumDensitySlope	Linear slope of regression fitted to the cumulative density of the radial density	none
pSkew	Skewness of the histogram of the radial trace	none
pSkew.1der	Skewness of the histogram of the first derivative of the radial trace	none
pSkew.2der	Skewness of the histogram of the second derivative of the radial trace	none
pKurt	Kurtosis of the histogram of the radial trace	none
pKurt.1der	Kurtosis of the histogram of the first derivative of the radial trace	none
pKurt.2der	Kurtosis of the histogram of the second derivative of the radial trace	none
pOWDensity	Mean density of the outer 25% of the radius	none
pOWDensitySD	Standard deviation of the outer 25% of the radius	none
pOWSlope	Linear slope of regression fitted to outer 25% of radial trace	none
pIWDensitySD	Standard deviation of the inner 25% of radius	none
pIWSlope	Linear slope of regression fitted to inner 25% of radial trace	none
pSD.ratio	pDensitySD / pOWDensitySD	none
pSD.ratio.IWOW	pIWDensitySD / pOWDensitySD	ln

Utilising these variables, two model formulations were pursued; step-wise multiple regression and random forests (Liaw and Wiener 2002) machine learning algorithms. Data from logs 1–12 only were used as these explained the population

of sawlogs (2.5-30m tree height) and excluded predominantly non-structural top logs. All analyses and reporting was done in R (R Core Team 2024) using RMarkdown (Allaire et al. 2024) within the RStudio environment (Posit team 2024).

The regression model was fitted using stepwise forward regression on all 29 variables. Variables identified as significant predictors in the data set were then used to fit models using a randomly selected set of 75% of the samples as a training set over 100 cycles of model fitting. Each cycle involved a different randomly selected sample set. The remaining 25% in each cycle were used to evaluate model performance. The model metrics of each fit were recorded and summarised.

For the random forest model, of the 29 independent variables generated for Log MOE and HM200 prediction, 18 variables (mtry in model formulation) were randomly selected at each split, in 500 trees (nTree). The training set used 75% of the observations, with the remaining 25% for model prediction. This model fitting was repeated 50 times using different, randomly selected training and test sets each time. Model metrics were recorded and summarised.

Results

Site effects on mean tree basic density and MoE

As an initial examination of site effects, the whole stem mean values of basic density, MoE and AWV were calculated by determining the under-bark volume of each log and weighting its value according to its contribution to the whole stem volume. The differences between site means was highly significant for stem volume, MOE and AWV (Fig. 3). The effect of stand age on stem volume is readily apparent, with the low stem volumes for the younger sites 821, 830, 833. The age effect on MOE and AWV is also visually apparent (Fig. 3c&d) with younger stands having significantly lower MOE and AWV values than the 26 year old trees at site 828.

Preliminary to exploring the within-tree variation patterns in MOE, the following analysis examined the inter-relationship of the potential drivers of tree and coupe variability in MOE with a view to identifying the dominant effects on stiffness using linear and linear mixed effects modelling (Gałecki and Burzykowski 2013). In addition to the site level variables described in Table 1, individual tree height and DBH were used in the analysis. A further variable called the “Dominance Index” was calculated as the individual tree DBH divided by the plot mean basal area. That is a less dominant tree is likely to grow taller relative to diameter, compared to more dominant trees in the plot, as it competes for light.

Following the assessment of a range of mixed effects and general linear models, the following linear model was found to best fit the data, with the effect on MOE assessed as:

$$TreeMeanMoE \approx \ StandAge + Stocking + TreeHeight + DBH + DominanceIndex$$

where:

- TreeMeanMoE is the volume weighted mean MOE of all the logs measured in each tree
- Stand Age is the time since planting in years
- Stocking is the stems per hectare at time of sampling
- Tree Height is the individual tree height in meters
- DBH is the individual over-bark diameter at breast height at the time of sampling
- Dominance Index is individual tree DBH (cm) divided by plot mean basal area (m2)

This assessment was based on AIC criteria (Akaike 1974; Gałecki and Burzykowski 2013). The main issue using linear mixed effects modelling was the relatively small number of plots (n = 13), relative to the fixed effects. The plot random effect explained zero variance.

All five predictors were statistically significant at the 0.05 level (Table 3), with DBH having a major effect; larger trees having lower MOE. All other predictors had a significant effect, while the effect of the intercept was not significant. Given the high collinearity between stand age, tree height and DBH, interactions were explored, as well as replacing these three with a single principal component, derived from principal components analysis, capturing their covariance. Based on model evaluation criteria, the above model resulted in lower AIC values and double the explained variance. Interaction terms were non-significant.

Table 3
Linear model of site factors driving variance in plot average tree MOE.

Variable	Estimate	Std.Error	df	t value
(Intercept)	-1.752	2.387	-0.734	0.466
Age	0.306	0.089	3.452	0.001
Stocking	0.003	0.001	2.995	0.004
Dominance Index	4.834	2.024	2.388	0.020
Tree height	0.181	0.054	3.365	0.001
DBH	-0.200	0.038	-5.284	0.000
R-squared	0.635			
Adj. R-squared	0.603			

Longitudinal variation in log MOE

The 2.5 m log length provided a relatively high resolution pattern of the longitudinal change in stiffness. An initial exploration of the data (Fig. 4a&c) revealed the increasing then decreasing trend in log MoE and acoustic wave velocity (AWV) with tree height. The generally lower values in the younger stands (821, 830, 833) are evident in their MoE and HM200 values as well as their fewer logs per stem. Maximum MoE values occurred around 10 metres above ground. Green density showed the greatest variability in the lower stem, presumably as a function of heartwood formation. The longitudinal patterns when expressed as a percentage of tree height (Fig. 4bd&f) showed maximum values of MoE and AWV between 20–40%. Expressing log values as percentages of tree height made the longitudinal patterns more consistent between sites, regardless of site age while retaining the variation in the y-intercept values.

What is evident in these patterns of variation is the potential for sampling around breast height to inform the properties of upper logs. Figure 5 shows the variance explained between the first log (0-2.5m stem height) and upper logs for both measured HM200 and Log MOE values. Above 20 metres the relationship is poor.

Prediction of log MoE by Resi

Orthogonal Resi traces taken from each disc provide a means of comparing Resi measures of basic density with the actual measured MOE values from individual logs. The two Resi derived metrics of density from each disc (sampling height) were averaged and compared with the actual log MOE values (Fig. 6a&b). Resi disc density explained 30% ($p < 0.001$) of the variance in the 590 measured log MOE values, where as the Resi-core density explained only 17% ($p < 0.001$). When the comparisons were restricted to the higher MOE logs lower in the stem (logs 3–6), that displayed a comparatively higher proportion of mature wood, these relationships strengthened to 42% and 28% variance explained respectively (Fig. 6c&d), and reduced the standard error of prediction accordingly.

The relationship between Resi density and log MoE was compared with groups defined by log number (distance from ground). The correlation was weaker in the first log, and tended to strengthen along the stem (Fig. 7). The general tendency for disc density and log MOE to decrease with tree height was also evident.

Modelling log MOE

A range of variables were extracted from the Resi trace (Table 2) and used to develop a predictive model of log MOE that explained more of the variance than basic density alone. Given the generally known radial pattern of MFA that decreases from pith to bark in a non-linearly in radiata pine (Evans et al. 2001), four parameter sigmoid curves were fitted to the radial patterns of the Resi data. Figure 8 illustrates 6 diverse traces where traces are taken from a range of log diameters and stem heights.

Table 2 lists each of the variables extracted from the trace as well as the statistical transformation used to best approximate a normal distribution. First and second derivatives of the trace were used to gain insight into the speed and rate of the changing amplitude values along the radius on the basis that this reflects to some extent changing cambial vigour potentially impacting MFA. Likewise the skewness and kurtosis of these variables might also explain variance affected by growth patterns independent of basic density. An important criterion (for routine commercial application) in this process was that all independent variables needed to be derived from the Resi trace directly so predictions could be determined from traces alone, without requiring the inclusion of other metrics. Similarly all variables needed to be calculated with minimal or no manual intervention (e.g. by identifying annual ring boundaries to estimate earlywood / latewood proportions) which would not be possible for a routine commercial application. The correlations among the dependent and independent variables (Fig. 9) shows the dependence of MoE on basic density, but also the mature wood density (pOWDensity, A) and the standard deviation of the radial density variation. HM200 values display a similar correlation pattern with a slightly stronger correlation with log diameter.

Stepwise multiple regression accounted for 51% of the variance in the log MoE using 13 of the 29 variables. Likewise 55% of the variance in the HM200 data was explained using 10 variables (Table 4); markedly more than density alone (Fig. 6).

Table 4
Summary metrics of stepwise regression to predict log MOE from Resi-derived variables.

Dataset	Count	minMOE	maxMOE	Range	adj.r2	Resid.se	Fstat	df	nVar	pValue
Log MOE	1,180	2.7	16.0	13.3	0.51	1.29	84.24	1,164	15	< 0.0001
HM200	1,180	1.7	4.2	2.5	0.55	0.25	121.85	1,167	12	< 0.0001

The results suggest the Resi-derived variables can explain commercially-useful levels of variance at the individual log level, but particularly at the plot mean level (Fig. 10), which is the intended commercial application.

To more fully explore the potential, prediction of log MOE in a set of logs not used in model development is required. A cross-validation approach was used, utilizing 100 cycles where 75% of the logs were randomly selected for model training, and the remaining 25% for prediction. On average, over the 100 cycles, 50.4% of the variance in log MOE was explained with an average standard error of prediction of 1.3 GPa.

Random Forest model

As an alternative to multiple regression, a random forest model was constructed utilising all 29 Resi-derived variables extracted from the trace. Models were fitted 50 times using a different, randomly selected training set each time, which was used to predict the values in the remaining set of samples. Again, 75% of the logs were allocated to the training set

and the remaining 25% allocated to the test set. The model fit metrics were summarised in Table 5. On average the random forest models explained approximately 5–6% more variance than the regression models.

Table 5
Average performance of the random forest model

Property	Units	Min.	Max.	Range	Test Set Mean	Predicted Mean	Variance explained (%)	R2.sd	RMSEP	SEP	Bias
LogMOE	GPa	2.70	16.0	13.32	7.96	7.96	57	0.04	1.21	1.21	0.01
HM200	km/sec	1.74	4.23	2.49	2.88	2.88	61	0.04	0.23	0.23	0.00

Discussion

The commercial dollar value of a given tree is a function of its volume, form and the properties of the wood within that volume. Commercially, volume and form are relatively easy to measure and are assessed in preharvest inventory to inform growers of expected yield. Internal properties are more difficult and expensive to quantify. Consequently they have generally not been included in the valuation process. That situation has slowly been changing following decades long research efforts being directed at non-destructive evaluation of wood properties (Evans 1994, 2006; Downes et al. 1997; Schimleck et al. 2019; Echols 1973). In recent years the implementation of resistance drilling has been adopted by many Australian plantation growers, to assess plantation wood quality with a view to better understanding its variation across the resource. Currently, these wood quality assessments are generally limited to breast height measures of average basic density and predicted stiffness. There is increasing potential to utilise longitudinal models of wood variability along the stem to be incorporated into yield table software. These approaches are particularly important for identifying better ways to quantify the effects and cost benefit of the large variety of silvicultural interventions and site characteristics that impact the volume of merchantable logs produced per hectare.

The ability of Resi to provide a robust estimate of basic density is well established (Downes et al. 2018; Gendvilas, Downes, et al. 2024; Sharapov et al. 2019). It is also understood that basic density is a strong indicator of log stiffness in close-to-harvest trees (Harris et al. 1976) where mature wood is a major contributor to log volume. Mature wood is characterized by generally higher density (compared to the juvenile core) and a lower microfibril angle (MFA). The data set contained here includes a large proportion of upper logs where the juvenile core (lower density and higher MFA) contributes a larger component to the log volume. This begs the question of whether other metrics can be extracted from the Resi trace that captures more of the variance that might be associated with the secondary wall microfibril angle and its radial pattern of variation, while being more independent of basic density.

Variation in measured MoE

Significant differences in average log and tree stiffness were observed among the study sites. Five available predictive metrics explained 60% of the variance in whole-stem MOE estimates in ways that are generally well understood.

- Stand age reflects the ratio of juvenile to mature wood within a log. By definition, juvenile wood comprises the first 10 rings from the pith in radiata pine (Moore and Cown 2017). Because juvenile wood has lower stiffness, a higher proportion of it reduces the overall log stiffness.
- Stocking influences how much growing space each tree receives, affecting its access to light, soil moisture, and nutrients. These factors, in turn, modify growth rates, and the ratio of height to diameter growth.
- Tree Height clearly influences the load experienced by the stem, affecting the wood properties needed to carry the load

- DBH: Increased stem diameter increases the ability of the stem to support the load, with leverage effects requiring less actual wood stiffness to support a given load in larger diameter stems
- Dominance index: The diameter of an individual stem relative to the site average basal area is indicative of the relative suppression (or dominance) of an individual tree. Competition for light will result in less dominant trees tending to have greater slenderness, with increased material stiffness of the stem wood to offset the reduced geometric stiffness resulting from smaller diameters.

In the present data set, no significant interactions among age, tree height or DBH were evident, yet each variable exerted a statistically significant effect on stem stiffness. Stem stiffness (flexural rigidity) is determined by the product of two factors; Young's modulus (material stiffness related to wood density) and the second moment of area (geometric property related to diameter) (Fournier et al. 2013; Downes and Turvey 1993; Downes et al. 1993). In this relationship stem diameter dominates, as the second moment of area for a cylindrical stem scales with diameter to the fourth power ($I \propto d^4$). Doubling the diameter makes the stem approximately 16 times stiffer structurally, all else being equal. Wood density correlates positively with Young's modulus (E). However, this relationship is roughly linear, where doubling wood density approximately doubles stem stiffness. Because diameter has a fourth-power effect while wood density has roughly a linear effect, diameter is the dominant factor in determining overall stem stiffness. A larger-diameter tree with lower-density wood can easily be stiffer than a small-diameter tree with high-density wood. Variation in stem taper affects the effective stiffness along the stem.

Longitudinal variation in Log MoE

The high resolution of the log MoE data (log length = 2.5m) allowed the marked and consistent pattern of MoE within individual tree stems to be observed. This pattern found log MoE to increase from the first log to a maximum in logs 2–5, before declining progressively in logs above that point. This non-linear pattern of change was more consistent when expressed as a percentage of stem height than when based on actual height. The pattern was also consistent between plots, albeit that the y-intercept differed between them. The tendency for younger age stands to have a lower y-intercept was evident. Xu and Walker (2004) noted the lower stiffness of the butt log in a mill study of 62 radiata pine stems, but found no decrease in stiffness with stem height above this point. However, given the dependence of stiffness on basic density and the well reported decrease in basic density with height in stem (Billard et al. 2021; Legg and Bradley 2016; Wassenberg et al. 2014), the patterns reported here are expected.

Predicting log MoE

Resistance drilling is now well accepted as a cost-effective indicator of basic density in standing trees (Downes et al. 2018; Downes et al. 2022; Schimleck et al. 2019; Gendvilas, Lee, et al. 2024; Lear et al. 2010; Gendvilas, Downes, et al. 2024). It is also well established that basic density is a major determinant of wood stiffness (Vikram et al. 2011; Yang and Evans 2003), albeit not the only one (Downes et al. 2002; Donaldson 2008; Lachenbruch et al. 2010a; Xu et al. 2004). The role of the contribution of secondary wall microfibril to explaining variance in MOE is well known (Vaněrek et al. 2017; Tamer and Fauziah 2013) and better captured by acoustic tools (Mason et al. 2017) such as the FibreGen HM200 instrument. However, there is also a strong correlation between HM200 and basic density and often a correlation between average MFA and basic density (Sheng-zuo et al. 2004; Lachenbruch et al. 2010b; Donaldson 2008) when examined across the radius (i.e. early wood to late wood and juvenile wood to mature wood). In the study reported here Resi predictions of basic density were moderately strongly correlated with MoE and HM200 values across all logs, and the strength of the relationship varied with distance along the stem. Previous work (Sharapov et al. 2019) had found resistance drilling amplitude to provide reasonable estimates of MOE, especially when combined with acoustic measurements (Brunetti et al. 2023).

A primary goal of this study was to determine whether the radial pith-to-bark Resi trace conveys information about modulus of elasticity (MOE) beyond what is captured by basic density alone. To investigate this, we extracted a suite of variables from the radial Resi trace that characterise its pattern. These included parameters derived from a four-parameter logistic curve Ratkowsky (1990) as well as descriptive metrics of the distribution and variability of density values along the trace. This approach builds on earlier work (Downes and Lausberg 2016), which used similar techniques to predict HM200 values in radiata pine logs.

Using cross-validated regression and random-forest models, we identified predictors that explained substantially more variance in log MOE than basic density (effectively DR) alone. The random-forest models outperformed conventional multiple-regression approaches. The resulting models are now accessible to commercial users of resistance-drilling technology through web-based trace-processing platforms. While confidence in the commercial use of either of these models can only be gained by application to independent data sets, subsequent evaluations have provided encouraging results (Downes unpublished data).

Conclusions

Log MOE varies systematically within tree stems across contrasting sites, increasing from the base and maximizing between 20% and 40% of tree height. There is a strong similarity of pattern between trees and sites, with marked differences in the starting MOE value at ground level. The average MOE of radiata pine tree stems at a given location can be estimated from site and growth metrics including stand age, stocking, plot average basal area, tree height and DBH. These explained 60% of the individual tree mean variance.

Predictive models of log MOE derived metrics automatically extracted from Resi traces, were able to explain over 50% of the variance in log MOE in independent test sets, with random forest models tending to explain 5–6% more variance than multiple regression models. These predictive models have been included in web-based Resi processing platforms accessed routinely by commercial grower operations. They are undergoing further validation and refinement as data becomes available.

Declarations

Conceptualization,G.M.D. methodology, G.M.D., R.M.; software, G.M.D.; formal analysis, G.M.D., R.M., V.G.; resources, K.A., R.M., G.M.D.; data curation, G.M.D.; writing—original draft preparation G.M.D.; writing—review and editing, D.J.L., V.G., R.M. and K.A.;visualization, G.M.D.; project administration, D.J.L.; funding acquisition, D.J.L. All authors have read and agreed to the published version of the manuscript.

Conflicts of Interest:

The authors declare that the research was conducted in the absence of any commercial or financial relationships that could be construed as a potential conflict of interest.

Funding:

This research was funded by Forest Quality Pty. Ltd. and Forestry and Wood Products Australia project “Assessing and managing mid-rotation wood quality in Australian softwood plantations to produce fit-for-purpose logs”. Project number: PNB548-2021. Tree harvest and infield data collection was funded by Timberlands Pacific Pty. Ltd.

Author Contribution

Conceptualization, G.M.D. methodology, G.M.D., R.M.; software, G.M.D.; formal analysis, G.M.D., R.M., V.G.; resources, K.A., R.M., G.M.D.; data curation, G.M.D.; writing—original draft preparation G.M.D.; writing—review and editing, D.J.L., V.G., R.M. and K.A.; visualization, G.M.D.; project administration, D.J.L.; funding acquisition, D.J.L. All authors have read and agreed to the published version of the manuscript.

Acknowledgement

This research was funded by Forest Quality Pty. Ltd. and Forestry and Wood Products Australia project “Assessing and managing mid-rotation wood quality in Australian softwood plantations to produce fit-for-purpose logs”. Project number: PNB548-2021. Tree harvest and infield data collection was funded by Timberlands Pacific Pty. Ltd.

Data Availability

Data are available from the corresponding author upon reasonable request. Our intention is to deposit data at Github in a publicly accessible repo. Timberlands Pacific in Tasmania provided all field sampling and data collection. Forest Quality undertook the data analysis which involved calculation of metrics used in model development. These metrics are described in the manuscript.

References

1. Akaike H (1974) A New Look at the Statistical Model Identification. IEEE Trans Autom Control 19(6):716–723. https://doi.org/10.1109/tac.1974.1100705
2. Allaire JJ, Yihui Xie C, Dervieux J, McPherson J, Luraschi K, Ushey A, Atkins et al (2024) Rmarkdown: Dynamic Documents for r. 2024. https://github.com/rstudio/rmarkdown
3. Bailleres H, Lee D, Kumar C, Psaltis S, Hopewell G (2019) and Loic Brancheriau. Improving Returns from Southern Pine Plantations Through Innovative Resource Characterisation. Report Nos. PNC361-1415. Forest & Wood Products Australia Limited. https://www.fwpa.com.au/images/resources/-2019/Final_Report_Southern_Pines_PNC361-1416.pdf
4. Barría Cristián, Sandoval Simón (2017) and Gerson Rojas. Uso Del Método de Resistografía Para La Predicción de La Densidad Básica de La Madera En Árboles En Pie de Pinus Radiata. Maderas. Ciencia y Tecnología, no. ahead (2017): 0–0. https://doi.org/10.4067/s0718-221x2017005000030
5. Bates D, Mächler M, Bolker B, Walker S (2015) Fitting Linear Mixed-Effects Models Using Lme4. J Stat Softw 67(1). https://doi.org/10.18637/jss.v067.i01
6. Beets PN, Mark O, Kimberley GR, Oliver, Pearce SH (2018) Predicting Wood Density of Growth Increments of Douglas-Fir Stands in New Zealand. N Z J Forest Sci 48(1). https://doi.org/10.1186/s40490-018-0112-z
7. Billard A, Bauer R, Mothe Frédéric, Colin F, Deleuze C, and Fleur Longuetaud (2021) Vertical Variations in Wood Basic Density for Two Softwood Species. Eur J For Res 140(6):1401–1416. https://doi.org/10.1007/s10342-021-01402-y
8. Bouffier L, Charlot Céline, Raffin A, Rozenberg P, and Antoine Kremer (2008) Can Wood Density Be Efficiently Selected at Early Stage in Maritime Pine (Pinus Pinaster Ait)? Ann For Sci 65(1):106–106. https://doi.org/10.1051/forest:2007078
9. Brunetti M, Aminti G, Vicario M, and Michela Nocetti (2023) Density Estimation by Drilling Resistance Technique to Determine the Dynamic Modulus of Elasticity of Wooden Members in Historic Structures. Forests 14(6):1107.

https://doi.org/10.3390/f14061107

10. Cown DJ, and J D Hutchison (1983) Wood Density as an Indicator of the Bending Properties of Pinus Radiata Poles. N Z J Forest Sci 13(1):87
11. Dahlen J, Auty D, Eberhardt TL, Schimleck L, Nawa RP (2023) Determination of Ring-Level Dynamic Modulus of Elasticity in Loblolly Pine from Measurements of Ultrasonic Velocity and Specific Gravity. Forestry 96(4):588–604. https://doi.org/10.1093/forestry/cpac063
12. Donaldson L (2008) Microfibril Angle: Measurement, Variation and Relationships a Review. IAWA J 29(4):345–386. https://doi.org/10.1163/22941932-90000192
13. Donaldson LA, Grace J, Downes GM (2004) Within-Tree Variation in Anatomical Properties of Compression Wood in Radiata Pine. IAWA J 25(3):253–271. https://doi.org/10.1163/22941932-90000364
14. Downes GM, Beckers EPJ, Turvey ND, Porada H (1993) Strength and Structure of Stems from Fast Grown Pinus Radiata. Trees 7(3). https://doi.org/10.1007/bf00199612
15. Downes GM, Lausberg M, Potts BM, Pilbeam DL, Bird M, Bradshaw B (2018) Application of the IML Resistograph to the Infield Assessment of Basic Density in Plantation Eucalypts. Australian Forestry 81(3):177–185. https://doi.org/10.1080/00049158.2018.1500676
16. Downes GM, Turvey ND (1993) Relationships Between Stem Structure and Bending Strength in Pinus Radiata Seedlings. Trees 7(2). https://doi.org/10.1007/bf00225474
17. Downes G, Drew D, Lee D (2020) Validated Softwood Stiffness Predictions Using IML-Resistograph and eCambium. Forest & Wood Products Australia: Melbourne, Australia, 2020
18. Downes GM (2023) User Guide to the Forest Quality Resistance Drilling Online Processing Platform. Unpublished, ahead of print, 2023. https://doi.org/10.13140/RG.2.2.11143.16801
19. Downes GM, Gwinyai Nyakuengama J, Evans R, Northway R, Blakemore P, Dickson RL, and Marco Lausberg (2002) Relationship Between Wood Density, Microfibril Angle and Stiffness in Thinned and Fertilized Pinus Radiata. IAWA J 23(3):253–265. https://doi.org/10.1163/22941932-90000302
20. Downes GM, Jonathan J, Harrington DM, Drew M, Lausberg P, Muyambo D, Watt, Lee DJ (2022) A Comparison of Radial Wood Property Variation on Pinus Radiata Between an IML PD-400 'Resi' Instrument and Increment Cores Analysed by SilviScan. Forests 13(5):751. https://doi.org/10.3390/f13050751
21. Downes G (2016) and Marco Lausberg. Evaluation of the RESI Software Tool for the Prediction of HM200 Within Pine Logs Sourced from Multiple Sites Across New Zealand and Australia. Unpublished, ahead of print, 2016. https://doi.org/10.13140/RG.2.2.13695.38560
22. Downes G, Lee D (2024) Report 32: Discussion Paper: Towards Improving the Prediction of Log MOE from Resi Traces. Report. University of the Sunshine Coast
23. Downes GM, Hudson IL, Raymond CA, Dean GH, Michell AJ, Schimleck LR, Evans R, Muneri A (1997) Sampling Plantation Eucalypts for Wood and Fibre Properties. January 1, 1997. https://doi.org/10.1071/9780643105287
24. Echols RM (1973) Uniformity of Wood Density Assessed from x-Rays of Increment Cores. Wood Sci Technol 7(1):34–44. https://doi.org/10.1007/bf00353377
25. Eckard JT, Isik F, Bullock B, Li B, and Marcia Gumpertz (2010) Selection Efficiency for Solid Wood Traits in Pinus Taeda Using Time-of-Flight Acoustic and Micro-Drill Resistance Methods. For Sci 56(3):233–241. https://doi.org/10.1093/forestscience/56.3.233
26. Elzhov TV, Katharine M, Mullen A-N, Spiess, Bolker B (2023) Minpack.lm: R Interface to the Levenberg-Marquardt Nonlinear Least-Squares Algorithm Found in MINPACK, Plus Support for Bounds. https://CRAN.R-project.org/package=minpack.lm

27. Evans R (1994) Rapid Measurement of the Transverse Dimensions of Tracheids in Radial Wood Sections from Pinus Radiata. Hfsg 48(2):168–172. https://doi.org/10.1515/hfsg.1994.48.2.168
28. Evans R (2006) Wood Stiffness by x-Ray Diffractometry. Characterization of the Cellulosic Cell Wall, April 5, 2006, 138–146. https://doi.org/10.1002/9780470999714.ch11
29. Evans R, Booker R, Paul Kibblewhite R (2001) Variation of Microfibril Angle, Density and Stiffness in Fifty Radiata Pine Trees. 55th Appita Annual Conference, Hobart, Australia 30 April-2 May 2001: Proceedings, 2001, 9–13
30. Fournier M, Dlouhá J, Jaouen G, Almeras T (2013) Integrative Biomechanics for Tree Ecology: Beyond Wood Density and Strength. J Exp Bot 64(15):4793–4815. https://doi.org/10.1093/jxb/ert279
31. Fundova I, Funda T, Harry X, Wu (2018) Using Resistograph Pilodyn PLOS ONE 13(9):e0204518. https://doi.org/10.1371/journal.pone.0204518. Non-Destructive Wood Density Assessment of Scots Pine (Pinus Sylvestris l.)
32. Fundova I, Funda T, Harry XW (2019) Non-Destructive Assessment of Wood Stiffness in Scots Pine (Pinus Sylvestris l.) and Its Use in Forest Tree Improvement. Forests 10(6):491. https://doi.org/10.3390/f10060491
33. Gałecki A (2013) and Tomasz Burzykowski. Linear Mixed-Effects Models Using r. Springer New York. https://doi.org/10.1007/978-1-4614-3900-4
34. Gendvilas V, Downes GM, Lausberg M, Harrington JJ, and David J. Lee (2024) Predicting Wood Density Using Resistance Drilling: The Effect of Varying Feed Speed and RPM. J Article Forests 15(4). https://doi.org/10.3390/f15040579
35. Gendvilas V, Lee DJ, Kain DP, Kumar C, Downes GM, Lausberg M, Jonathan JH (2024) Predicting Wood Density Using Resistance Drilling: The Effect of Instrument and Operator. Forests 15(1):157. https://doi.org/10.3390/f15010157
36. Gil-Moreno, David JP, MClean, and Dan Ridley-Ellis (2023) Models to Predict the Radial Variation of Stiffness, Strength, and Density in Planted Noble Fir, Norway Spruce, Western Hemlock, and Western Red Cedar in Great Britain. Ann For Sci 80(1). https://doi.org/10.1186/s13595-023-01214-7
37. Gwaze D, and Aaron Stevenson (2008) Genetic Variation of Wood Density and Its Relationship with Drill Resistance in Shortleaf Pine. South J Appl For 32(3):130–133. https://doi.org/10.1093/sjaf/32.3.130
38. Harris J, Maddern RN, James, Collins MJ (1976) Case for Improving Wood Density in Radiata Pine. N Z J Forest Sci 5(3):347–354
39. Icel B (2025) Non-Destructive Estimation of Wood Density in Standing Pinus Brutia Trees Using the Drilling Resistance Method: Results and Insights. Maderas Ciencia y Tecnología 27:e4025 (December 2025. https://doi.org/10.22320/s0718221x/2025.40
40. Isik F, Li B (2003) Rapid Assessment of Wood Density of Live Trees Using the Resistograph for Selection in Tree Improvement Programs. Can J For Res 33(12):2426–2435. https://doi.org/10.1139/x03-176
41. Kennedy RW (1995) Coniferous Wood Quality in the Future: Concerns and Strategies. Wood Sci Technol 29(5). https://doi.org/10.1007/bf00202581
42. Kumar C, Psaltis S, Bailleres H, Turner I, Brancheriau L, Hopewell G, Carr EJ, Farrell T, and David J. Lee (2021) Accurate Estimation of Log MOE from Non-Destructive Standing Tree Measurements. Ann For Sci 78(1). https://doi.org/10.1007/s13595-021-01031-w
43. Lachenbruch B, Moore JR, and Robert Evans (2011) Radial Variation in Wood Structure and Function in Woody Plants, and Hypotheses for Its Occurrence. https://doi.org/10.1007/978-94-007-1242-3_5. Springer Netherlands
44. Lachenbruch B, Johnson GR, Downes GM, Evans R (2010a) Relationships of Density, Microfibril Angle, and Sound Velocity with Stiffness and Strength in Mature Wood of Douglas-Fir. Can J For Res 40(1):55–64. https://doi.org/10.1139/x09-174

45. Lachenbruch B, Johnson GR, Downes GM, and R. Evans (2010b) Relationships of Density, Microfibril Angle, and Sound Velocity with Stiffness and Strength in Mature Wood of Douglas-Fir. Can J For Res 40(1):55–64. https://doi.org/10.1139/x09-174
46. Lear G, Kasal B, Anthony R (2010) Resistance Drilling. Springer Netherlands. https://doi.org/10.1007/978-94-007-0560-9_5
47. Lee D, Downes G, Lausberg M, Gendvilas V, Harrington J, Rawley B, Dominic K, Drew D, and Chandan Kumar (2024) Assessing and Managing Mid-Rotation Wood Quality in Australian Softwood Plantations to Produce Fit-for-Purpose Logs. Report Nos. PNB548-2021. Forest & Wood Products Australia Limited. https://fwpa.com.au/report/assessing-managing-mid-rotation-wood-quality-in-australian-softwood-plantations/
48. Legg M, and Stuart Bradley (2016) Measurement of Stiffness of Standing Trees and Felled Logs Using Acoustics: A Review. J Acoust Soc Am 139(2):588–604. https://doi.org/10.1121/1.4940210
49. Liaw A (2002) and Matthew Wiener. Classification and Regression by randomForest. 2 (2002): 18–22. https://CRAN.R-project.org/doc/Rnews/
50. Mason EG, Hayes M, and Nigel Pink (2017) Validation of Ultrasonic Velocity Estimates of Wood Properties in Discs of Radiata Pine. N Z J Forest Sci 47(1). https://doi.org/10.1186/s40490-017-0098-y
51. Moore JR, and Dave J. Cown (2017) Corewood (Juvenile Wood) and Its Impact on Wood Utilisation. Curr Forestry Rep 3(2):107–118. https://doi.org/10.1007/s40725-017-0055-2
52. Moore JR, Dave J, Cown, Russell BMK (2014) Modelling Microfibril Angle Variation in New Zealand-Grown Radiata Pine. N Z J Forest Sci 44(1). https://doi.org/10.1186/s40490-014-0025-4
53. de Pádua FA (2019) João Otávio Poletto Tomeleri, Mariana Pires Franco, José Reinaldo Moreira da Silva, and Paulo Fernando Trugilho. Recommendation of Non-Destructive Sampling Method for Density Estimation of the Eucalyptus Wood. Maderas. Ciencia y Tecnología, no. ahead (2019): 0–0. https://doi.org/10.4067/s0718-221x2019005000412
54. Posit team (2024) RStudio: Integrated Development Environment for r. (Boston, MA), 2024. http://www.posit.co/
55. Pot G, Viguier J, and Anders Olsson (2025a) Evaluating Distance to the Pith as a Parameter for Strength Grading of Douglas Fir (Pseudotsuga Menziesii (Mirb.) Franco). Forests 16(3):504. https://doi.org/10.3390/f16030504
56. Pot G, Viguier J, and Anders Olsson (2025b) Evaluating Distance to the Pith as a Parameter for Strength Grading of Douglas Fir (Pseudotsuga Menziesii (Mirb.) Franco). Forests 16(3):504. https://doi.org/10.3390/f16030504
57. R Core Team (2024) R: A Language and Environment for Statistical Computing. R Foundation for Statistical Computing, Vienna, Austria. https://www.R-project.org/
58. Ratkowsky DM Handbook of Nonlinear Regression Models., Dekker M (1990) https://openlibrary.org/books/OL2205492M/Handbook_of_nonlinear_regression_models
59. Schimleck L, Dahlen J, Apiolaza LA, Downes G, Emms G, Evans R, Moore J, Pâques L, Van den Bulcke J, Wang X (2019) Variation Forests 10(9):728. https://doi.org/10.3390/f10090728. Non-Destructive Evaluation Techniques and What They Tell Us about Wood Property
60. Sharapov E, Brischke C, Militz H, and Elena Smirnova (2019) Prediction of Modulus of Elasticity in Static Bending and Density of Wood at Different Moisture Contents and Feed Rates by Drilling Resistance Measurements. Eur J Wood Wood Product 77(5):833–842. https://doi.org/10.1007/s00107-019-01439-2
61. Sheng-zuo F, Yang Wen-zhong, and, Fu Xiang-xiang (2004) Variation of Microfibril Angle and Its Correlation to Wood Properties in Poplars. J Forestry Res 15(4):261–267. https://doi.org/10.1007/bf02844949
62. Šilinskas B, Linkevičius E, Beniušienė L, Aleinikovas M, Zeleniakienė I, Škėma M, and Karol Tomczak (2026) The Wood Density of Pure and Mixed Norway Spruce, Scots Pine, and Silver Birch Stands in Lithuania Using IML Resi. Forests 17(3):376. https://doi.org/10.3390/f17030376

63. Singh KP, Iskandar Z, Siregar, Jupiter IM, Abad, and Lina Karlinasari (2023) Non-Destructive Modeling Using a Drilling Resistance Tool to Predict Wood Basic Density of Standing Trees in a Eucalypts Plantation in North Sumatra, Indonesia. Biodiversitas J Biol Divers 23(12). https://doi.org/10.13057/biodiv/d231217
64. Tamer A, Fauziah A (2013) Cellulose Microfibril Angle in Wood and Its Dynamic Mechanical Significance. https://doi.org/10.5772/51105. InTech
65. Todoroki CL, Eini C, Lowell, Filipescu CN (2021) Wood Density Estimates of Standing Trees by Micro-Drilling and Other Non-Destructive Measures. New Zealand Journal of Forestry Science 51 (June 2021). https://doi.org/10.33494/nzjfs512021x74x
66. Vaněrek J, Martinek Radomír, Čada P (2017) and Pavel Kuklík. The Influence of Microfibril Angle on the Wood Stiffness Parameters. Procedia Engineering 195 (2017): 259–264. https://doi.org/10.1016/j.proeng.2017.04.552
67. Vikram V, Cherry ML, Briggs D, Cress DW, Evans R, Howe GT (2011) Stiffness of Douglas-Fir Lumber: Effects of Wood Properties and Genetics. Can J For Res 41(6):1160–1173. https://doi.org/10.1139/x11-039
68. Vlad R, Pei G, Sidor CG, Cuciurean C, Ispravnic A, and Gheorghe Stefan (2022) Assessing Standing-Tree Wood Density by Microdrilling in Tending Forestry Work Carried Out on Norway Spruce (Picea Abies (l.) h. Karst). Stands Forests 13(9):1450. https://doi.org/10.3390/f13091450
69. Waghorn MJ, Euan G, Mason, Watt MS (2007) Influence of Initial Stand Density and Genotype on Longitudinal Variation in Modulus of Elasticity for 17-Year-Old Pinus Radiata. For Ecol Manag 252(1–3):67–72. https://doi.org/10.1016/j.foreco.2007.06.019
70. Wassenberg M, Chiu H-S, Guo W, and Heinrich Spiecker (2014) Analysis of Wood Density Profiles of Tree Stems: Incorporating Vertical Variations to Optimize Wood Sampling Strategies for Density and Biomass Estimations. Trees 29(2):551–561. https://doi.org/10.1007/s00468-014-1134-7
71. Watt MS, Garnett BT, Walker JCF (1996) The Use of the Pilodyn for Assessing Outerwood Density in New Zealand Radiata Pine. For Prod J 46(11/12):101
72. Watt MS, Zoric B, Kimberley MO, and Jonathan Harrington (2011) Influence of Stocking on Radial and Longitudinal Variation in Modulus of Elasticity, Microfibril Angle, and Density in a 24-Year-Old Pinus Radiata Thinning Trial. Can J For Res 41(7):1422–1431. https://doi.org/10.1139/x11-070
73. Xu P, Donaldson L, Walker J, Evans R, and Geoffrey Downes (2004) Effects of Density and Microfibril Orientation on the Vertical Variation of Low-Stiffness Wood in Radiata Pine Butt Logs. Holzforschung 58(6):673–677. https://doi.org/10.1515/hf.2004.122
74. Xu P, Walker JCF (2004) Stiffness Gradients in Radiata Pine Trees. Wood Sci Technol 38(1):1–9. https://doi.org/10.1007/s00226-003-0188-2
75. Yang JL, Evans R (2003) Prediction of MOE of Eucalypt Wood from Microfibril Angle and Density. Holz Als Roh- Und Werkst 61(6):449–452. https://doi.org/10.1007/s00107-003-0424-3
76. Yao J, Zhao Y, Lu J, Liu H, Wu Z, Song X, Li Z (2024) Research on the Wood Density Measurement in Standing Trees Through the Micro Drilling Resistance Method. Forests 15(1):175. https://doi.org/10.3390/f15010175

Figures

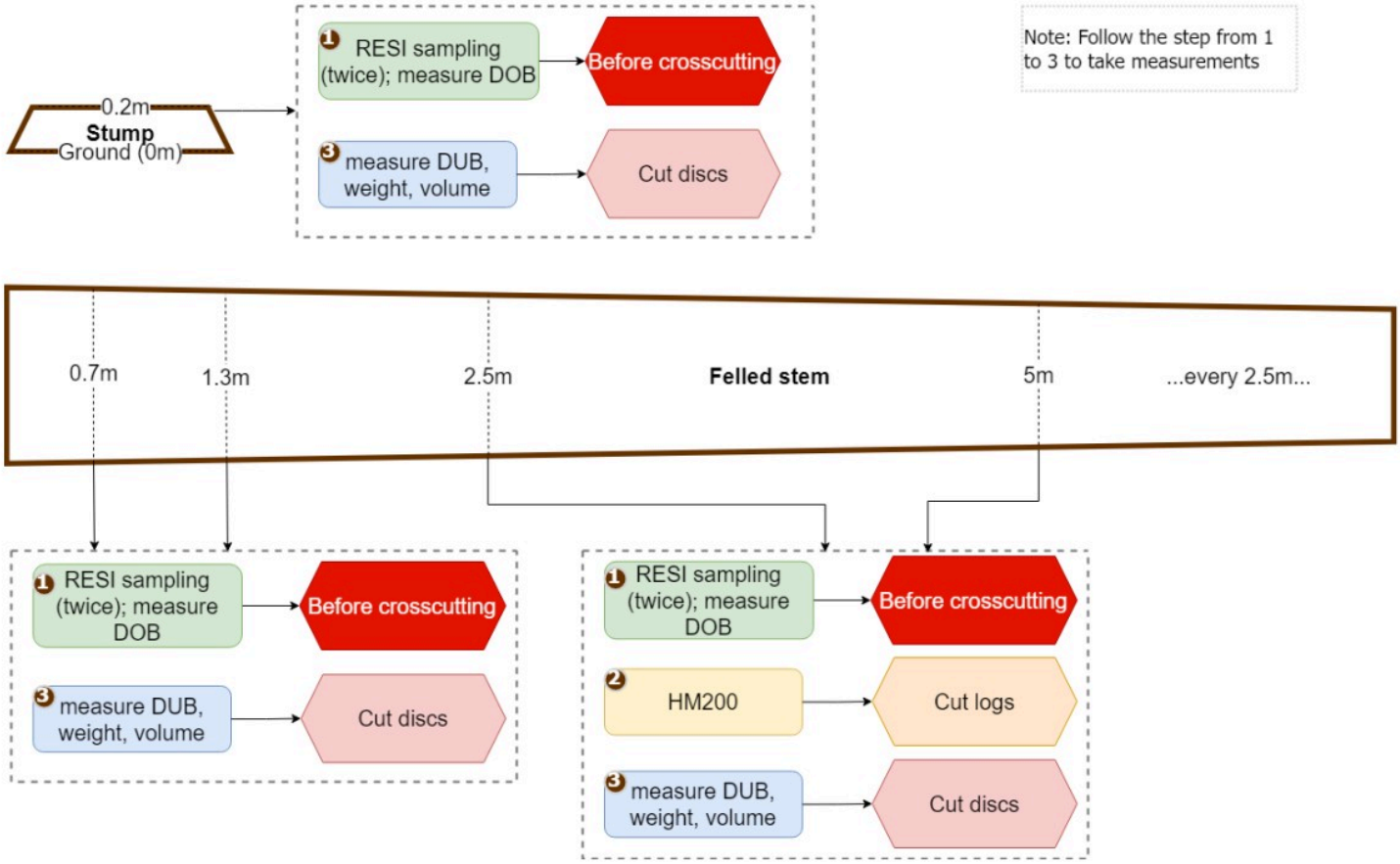


Figure 1

Each stem was sampled at multiple heights using Resi and bucked into logs from which discs HM200 values were recorded. Cross section discs were sampled from each Resi sampling point.

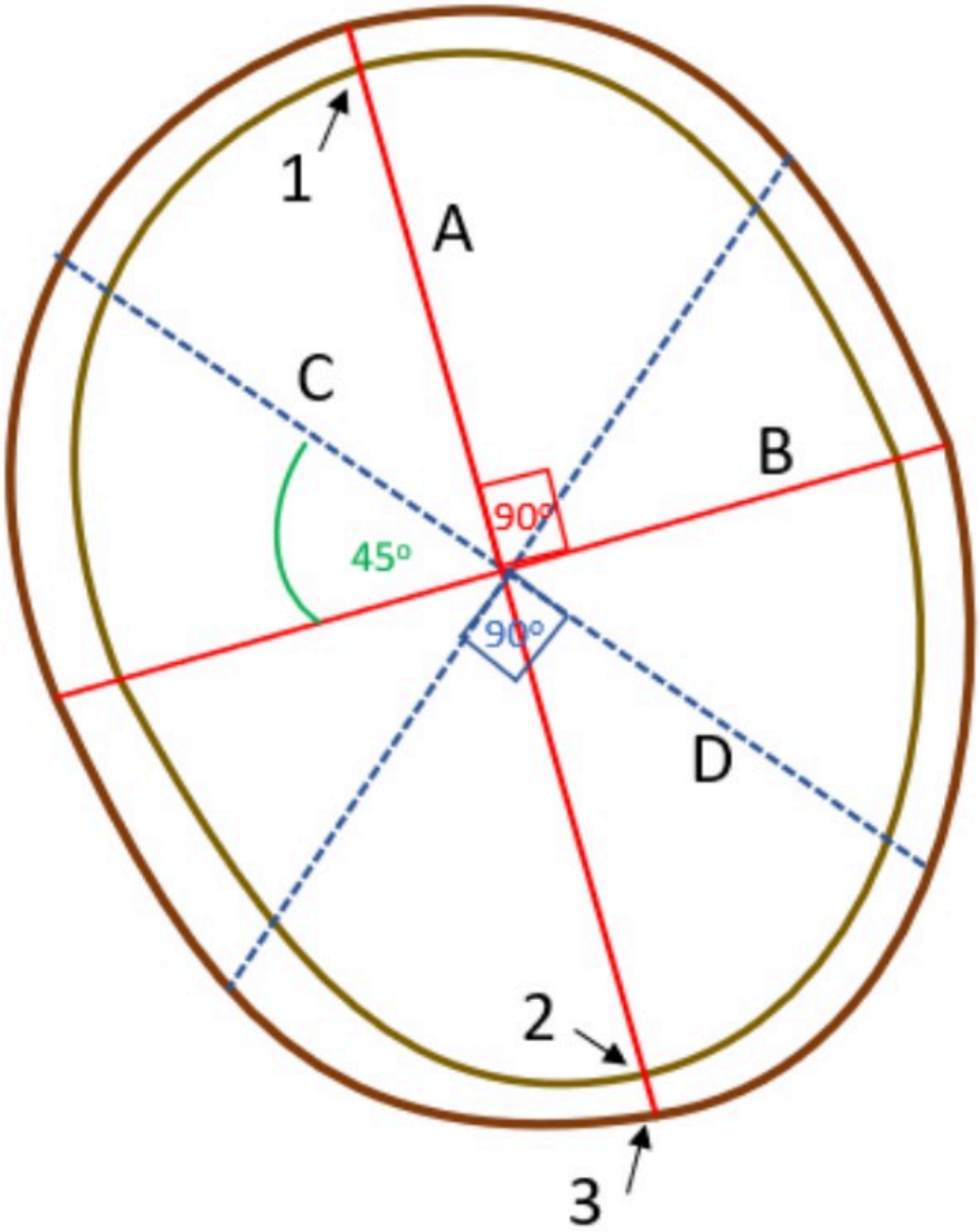


Figure 2

Over and underbark diameter measurement along lines A and B indicating the maximum and minimum diameters. Blue dashed lines show the direction of the Resi trace sampling points, effectively the points of minimal diameter variation.

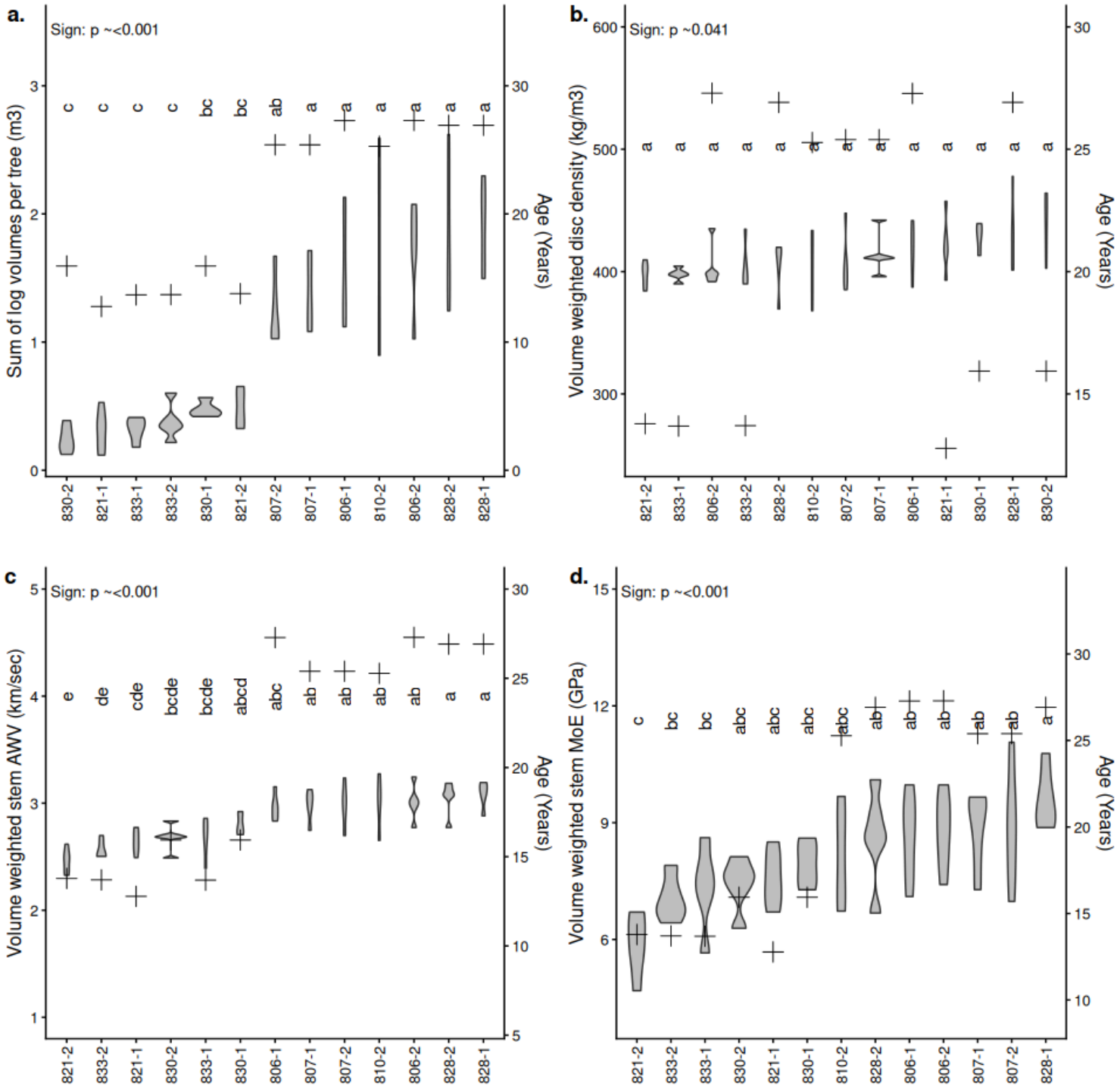


Figure 3

Calculated log weighted means for (a) total log volume per tree, and volume weighted (b) disc density, (c) acoustic wave velocity and (d) stiffness. (cross indicates the age in years at sampling.)

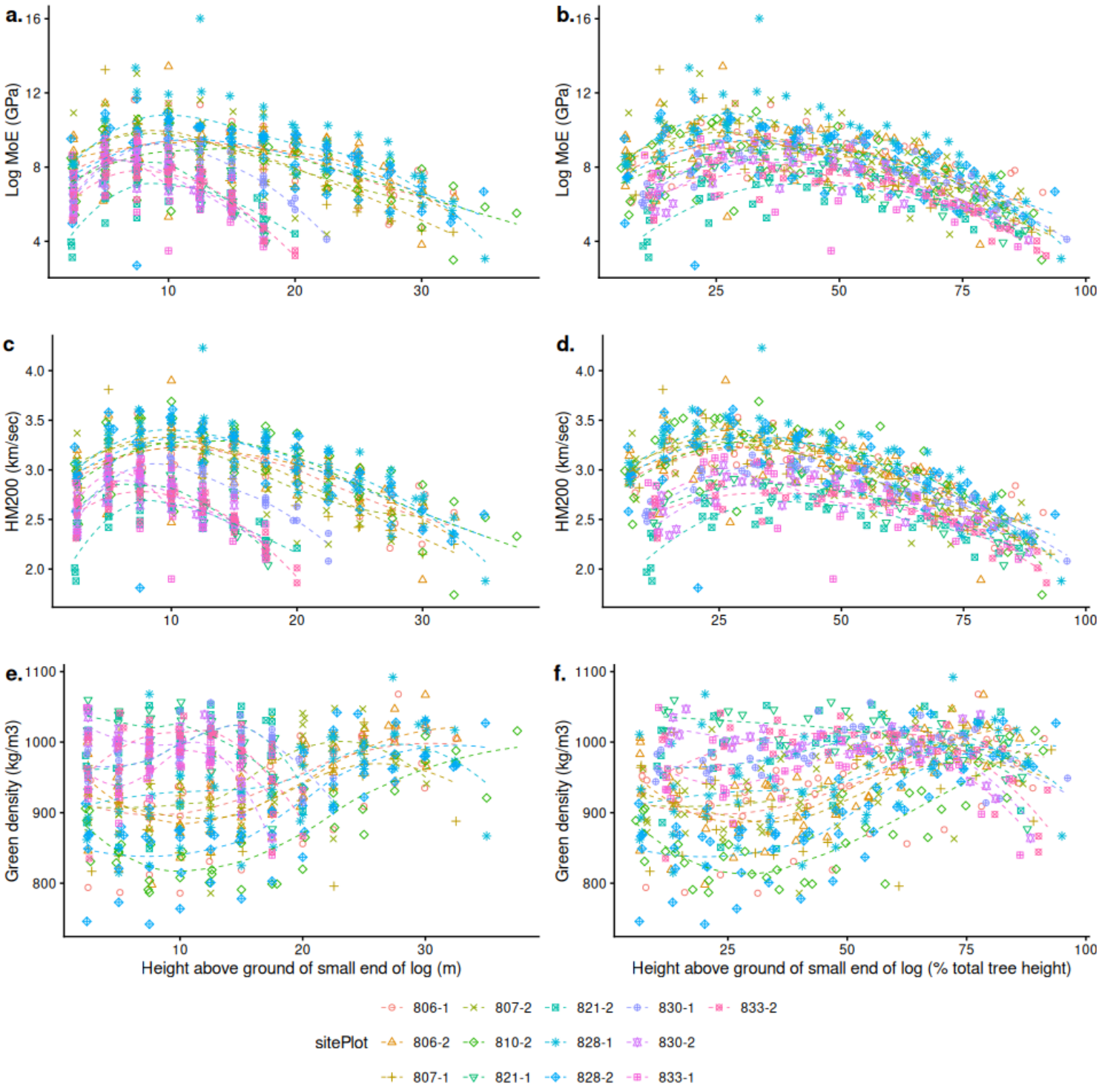


Figure 4

Log MoE (a,b) increased then decreased with tree height as did acoustic wave velocity (c,d). Green density (e,f) was most variable in the lower stem indicating the variability in heartwood content. Dashed lines indicated a fitted loess smooth using a span of 0.3.

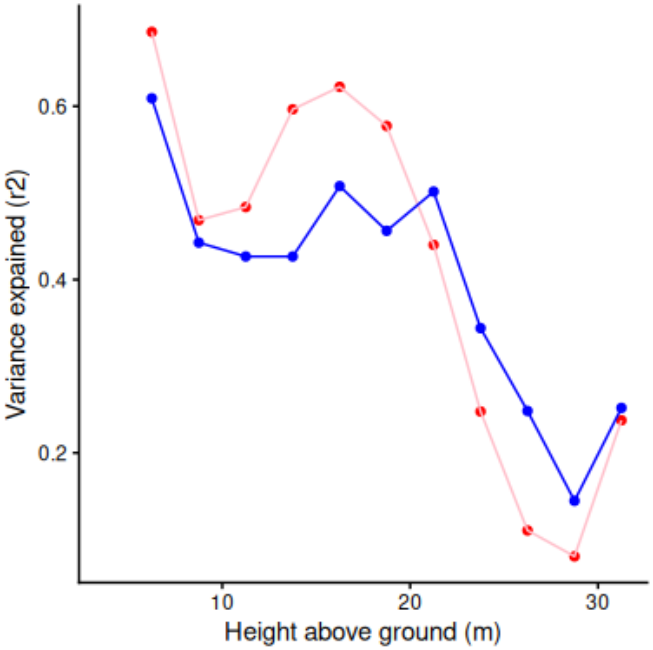


Figure 5

The variance explained in upper log MOE (blue) and AWV (red) by logs at the base of the stem decreased with height above ground when assessed across all sites and trees.

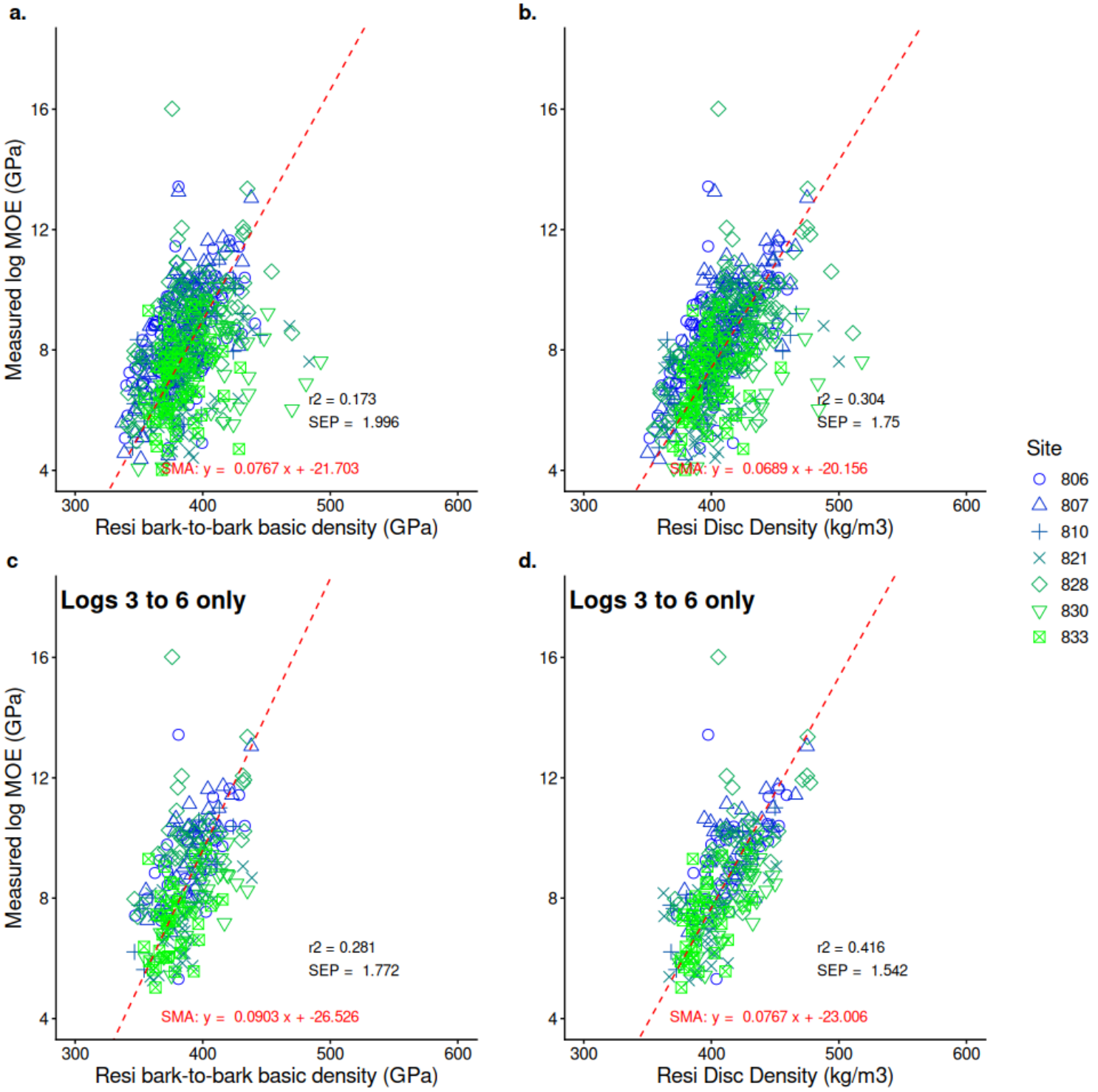


Figure 6

Measured log MoE across all trees and stem heights were compared with Resi-predicted metrics of mean (a) bark-to-bark density and (b) disc density. When the logs were restricted to between 7.5 and 15 meters the correlations strengthened to (c) 28% and (d) 42% explained variance respectively.

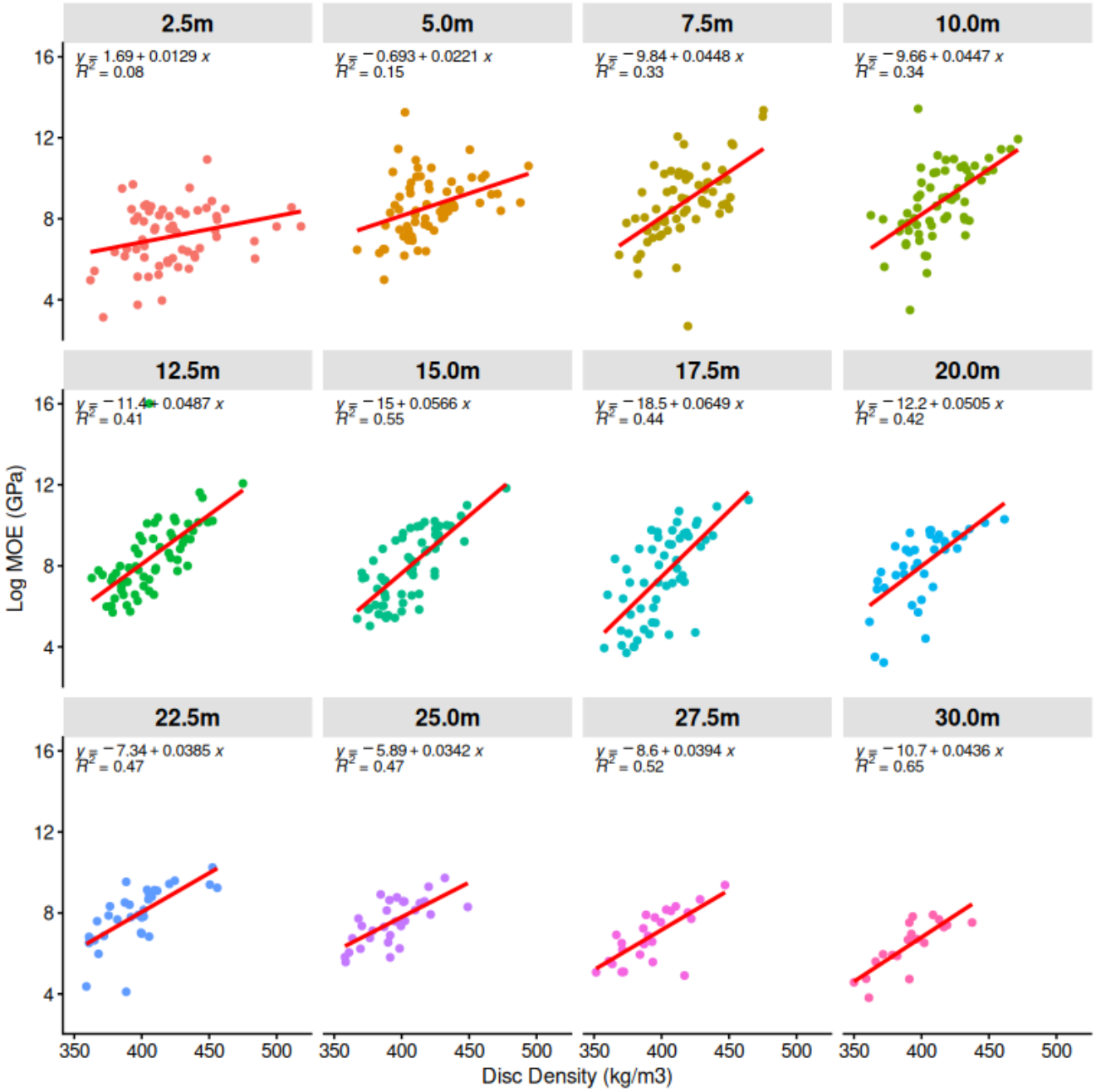


Figure 7

Disc density calculated from Resi traces from the disc sampled from the small end of logs were used to predict MOE of individual logs.

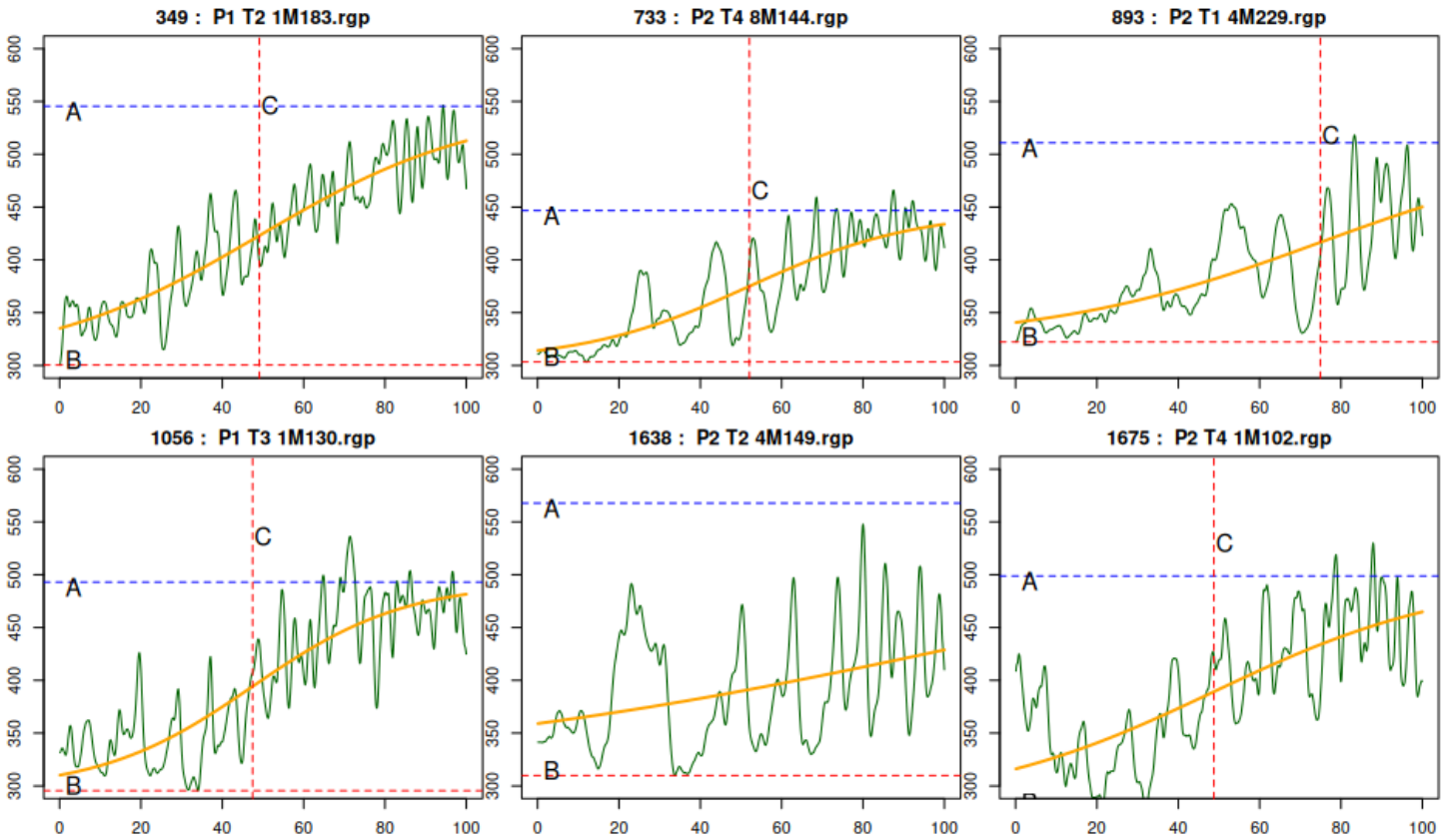


Figure 8

Sigmoid curves fitted to six of the individual radii derived from Resi traces at 0.1% intervals.

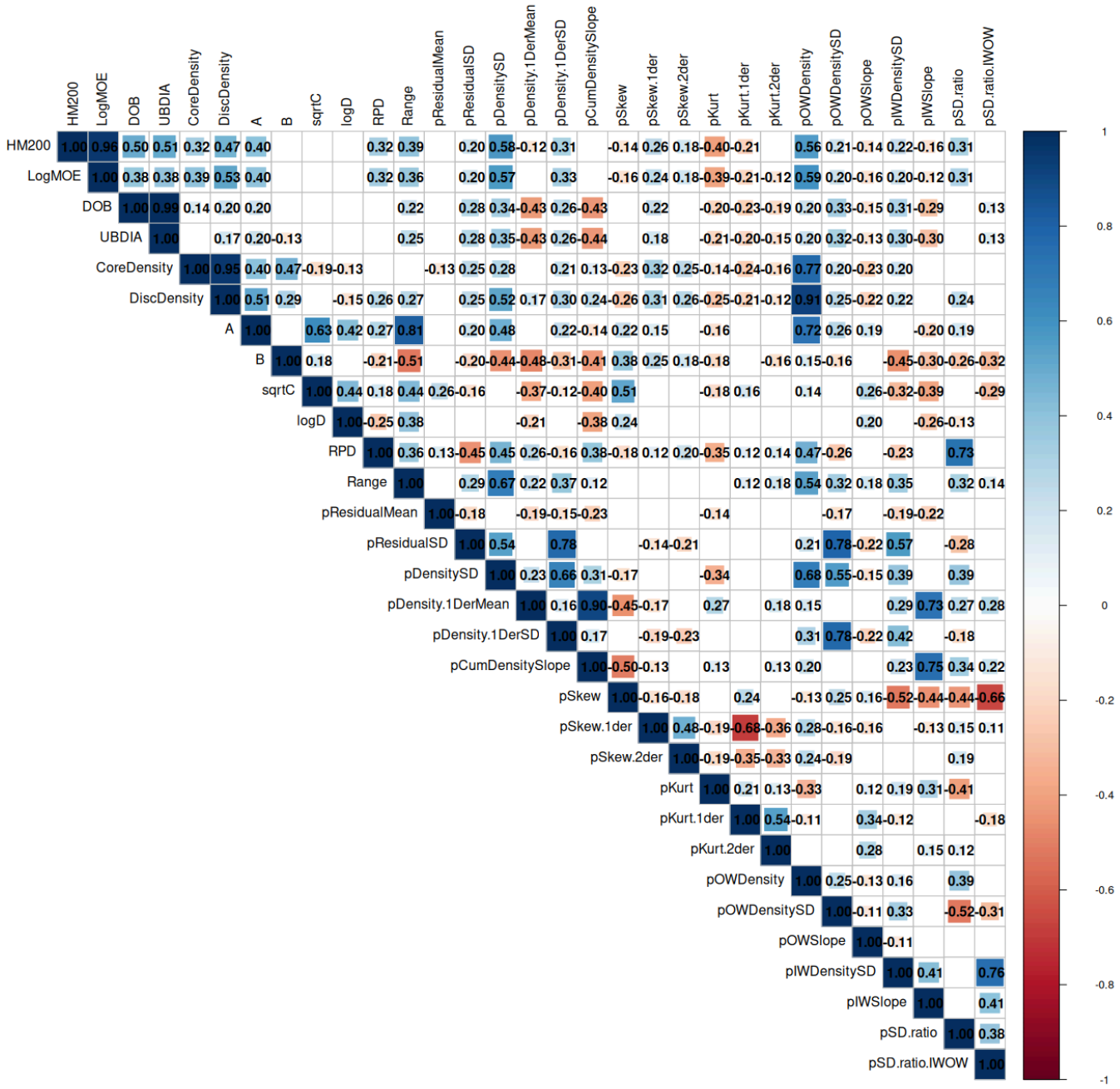


Figure 9

Correlation plot illustrating the stength and direction of correlation among the dependent variables. Only correlations significant at p<0.001 are shown (n=1180)

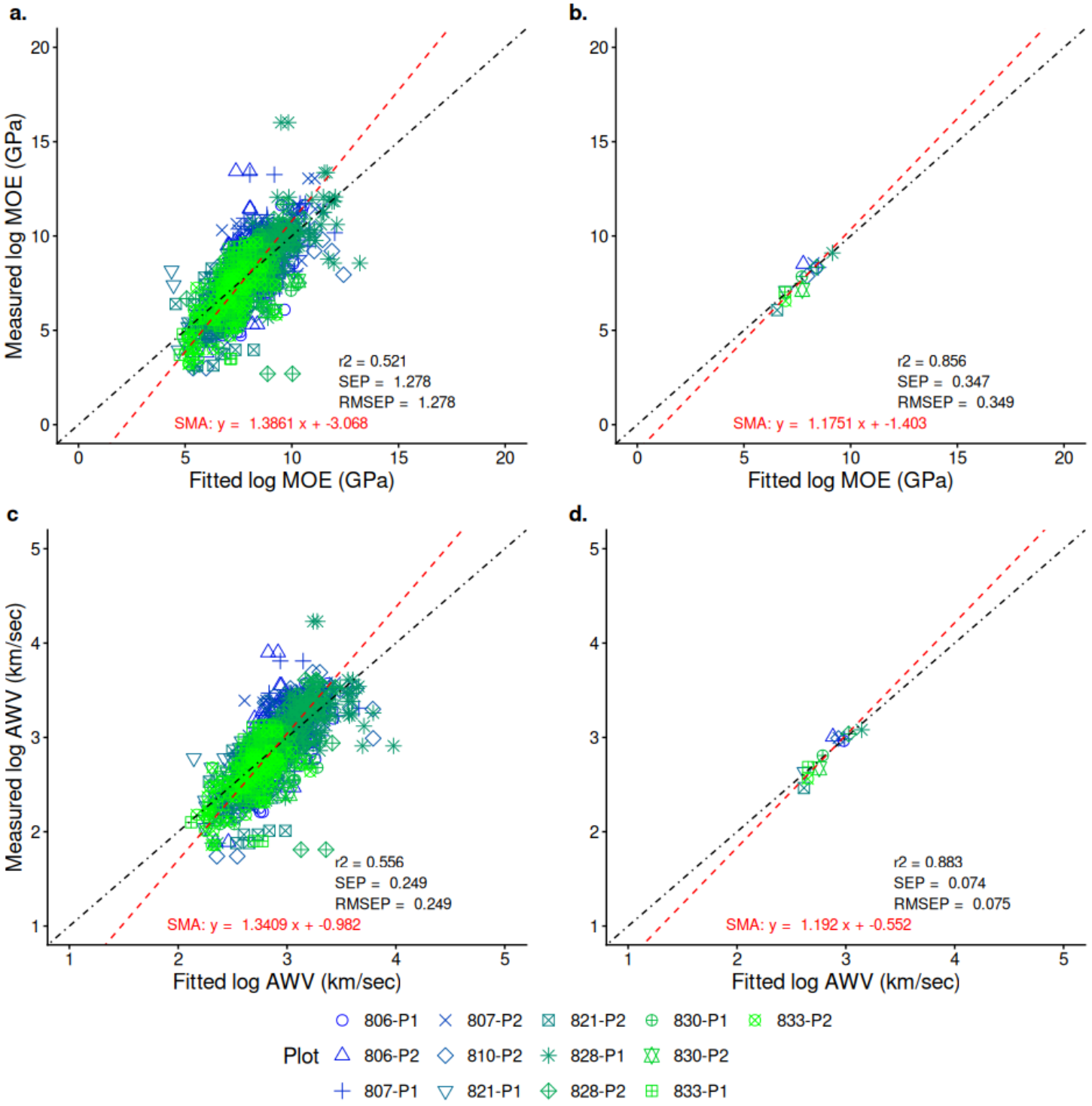


Figure 10

The multiple regression model explained 52% of the variance in log Moe at (a) individual log level and (b) 86% at the plot mean level. HM200 values were slightly better predicted at (c) 56% among logs and (d) 88% among plot means.